A comparison study on methanol reforming catalysts for on-board hydrogen generation

Yanjing Su[1a*], Jiao Yu[1b*], Jianyue Shen[2c*]

[1] Suzhou Qingjie Power Technology Co., Ltd, SuZhou200240, China
[2] Shanghai Palcan New Energy Technology Co., Ltd, Shanghai201108, China

Abstract—In hydrogen energy applications, methanol is the best fuel that can effectively solve the problem of the storage and transportation of hydrogen. The lowest reforming temperature among hydrocarbons also makes it the best fuel for hydrogen generation. This paper aimed to study and compare four methanol-reforming catalysts and screen the best one suitable for the on-board hydrogen generation system. In this study, the in-house single-tube reactor, which can precisely control the temperature by a multistage heater, was applied to study the catalyst performance. Physical and chemical properties of the catalyst, such as methanol conversion rate, hydrogen generation rate, CO selectivity at a different liquid hourly space velocity (LHSV), catalyst density, and optimum reaction temperature, were also systematically studied. The hydrogen generation rate per unit mass of the WEF catalyst is the highest, which reached 0.122 $g/h \cdot g_{cat}$ in 9.23 h^{-1} LHSV. And the methanol conversion rate in 7.72 h^{-1} LHSV is 96.74%, and somewhat below the BSF catalyst (97.90% in 7.55 h^{-1} LHSV). The study indicated that the catalyst made by WEF is the best catalyst for on-board hydrogen generation when comprehensively considering the requirement including the performance and vibration resistance. At the end of this paper, the optimized direction of the four catalyzers is also specified.

1. Introduction

Hydrogen is considered an environmentally friendly energy source due to its carbon-free properties. However, hydrogen has much less volume energy density (Wh/L) than other fuels (it is much less dense than other hydrocarbon and alcohol fuels under standard temperature and pressure conditions). There are still many problems to solve in high-pressure storage, low-temperature liquid storage, compound storage, and other methods [1-2], which caused many difficulties in the practical application of hydrogen. Therefore, by reforming natural gas, ethanol, methanol, dimethyl ether, gasoline, diesel, and so on into hydrogen-rich gas, the realization of online generation and use of hydrogen has gotten much attention.

As a hydrocarbon with only one carbon atom, methanol has the highest hydrogen-carbon ratio among the fuels that can generate hydrogen by the reforming reaction. Also, because of the lack of C=C bond [3], it could convert into hydrogen gas at low temperatures (200 ℃~300 ℃), which has considerable advantages over other hydrocarbons (such as methane: conversion temperature 800 ℃~1000 ℃ [4]; ethanol: the conversion temperature is more than 600 ℃ [5]).

The route of methanol-reforming nowadays is divided into four ways: Methanol Steam Reforming (MSR), Partial Oxidation of Methanol (POM), Autothermal Reforming of Methanol (ATRM), and Methanol Decomposition (MD) [6]. Methanol steam reforming has attracted much attention because of its higher efficiency and lower energy consumption [7]. The existence of the catalyst for methanol steam reforming makes the reaction pathway change, thus reducing the activation energy of the reaction and speeding up the chemical reaction. The commonly used MSR reaction catalysts mainly include copper-based and group VIII metal-based catalyzers [8].

Copper-based catalysts are more conducive to generating H_2 and CO_2 than most group VIII-X metallic element catalysts [9]. But there are still many problems in copper catalysts resulting in the degradation of performance, such as being more likely to suffer sintering, being more sensitive to sulfur and oxygen, and having much easier spontaneous combustion [6]. Adding auxiliaries can improve the stability of the copper-based catalyst, and the most commonly used auxiliaries are ZnO, ZrO_2, CeO_2, $Al2O_3$, etc. The catalyst with a spinel structure has also proven effective in improving the reforming performance [6]. Fasanya et al. [10] reported the performance of a nanostructured Cu-Zn catalyst with an alcohol-water ratio of 0.8. No CO was generated when the catalyst was tested at 180 ℃~230 ℃, indicating its potential in low CO application. Zhao et al. [11] investigate the Ti-modified $Cu/\gamma\text{-}Al_2O_3/Al$ catalyst prepared by the anodic oxidation method. The addition of Ti improved the dispersion of copper and increased the adsorption capacity of water and methanol. The co-existence of Ti^{4+} and Ti^{3+} also improves the redox properties of copper. When formulated as $CuTi_{1.9}/\gamma\text{-}Al_2O_3/Al$, the methanol conversion rate reached 100%.

[a*]yanjing_su@foxmail.com, [b*]george.yu@palcan.com.cn, [c*]jshen@palcan.com.cn

© The Authors, published by EDP Sciences. This is an open access article distributed under the terms of the Creative Commons Attribution License 4.0 (https://creativecommons.org/licenses/by/4.0/).

Chen et al. [12] developed a Cu-Zr component catalyst with Attapulgite-based Zeolite (AZ) as the support for the MSR reaction. The MSR activity tests showed that the microporous and mesoporous channels synthesized in AZ could improve the catalytic performance by promoting heat and mass transfer. Zr Addition significantly increased the distribution of active metal particles and the metal surface area and also promoted the formation of Cu^0/Cu^+-ZrO_xH_y interface sites. The synergistic effect above can inhibit the sintering and carbon deposition of active metals and promote the oxidation of intermediate products and the water vapor transformation reaction.

Pt and Pd-based catalysts are studied extensively among Group VIII metal-based catalysts. Compared with copper-based catalysts, they have excellent thermal stability, so there are fewer effects of being sintered (the most fundamental reason for performance attenuation). However, these catalysts require a higher operating temperature, and then the higher content of CO in the reforming gas was unavoidable. ZnO, ZrO_2, CeO_2, and Al_2O_3 also be commonly used for modifying group VIII metal-based catalysts [6,8]. Liu etc. [13] reported a $PdZn_\beta$ alloy catalyst load on $ZnAl_2O_4$ with an excellent CO_2 selectivity when palladium content is 1000ppm (97%). Kim et al. [14] find that Ru doping in Pd/Al_2O_3 can promote the methanol steam reforming reactions. Compared with Pd/Al_2O_3, adding Ru in $Pd/Ru/Al_2O_3$ can effectively improve its catalytic capacity. Further study showed that the main reason for the improvement was that the formation of Pd-Ru alloy reduced the size of Pd particles, which further improved the dispersion of Pd in the catalyst.

In this paper, two types of commercialized copper-based catalyzers (BSF and CLN), a platinum-based catalyst (WEF) and a self-developed copper-based catalyst (JSU), were systematically studied based on the application of vehicle catalysts for methanol-reforming. Considering the onboard reforming system used for hydrogen generation, the catalyst inside should be lightweight, energy-saving, and have better shock resistance to withstand a harsher working environment. Through the systematic analysis of the density of each catalyst, the optimal working temperature, reforming performance, and other parameters, it is found that the WEF type of platinum-based methanol reforming catalyst based on FeCrAl wire carrier is relatively more suitable for the use of the vehicle-mounted methanol-reforming system. At the same time, the paper puts forward the direction of further improvement for the four kinds of catalysts. The results laid a foundation for vehicle-mounted methanol reforming catalysts and systems.

2. Experimental

2.1 Experimental Instrument

The Steam Reformer (STR) used in this experiment has several heating rings, and it can control the temperature by multistage heating. Due to the order, the carrier (catalyst) close to the inlet may catalyze more methanol-water steam, resulting in a temperature difference between the different sites in the STR tube. The design of the STR can solve the problem dexterously, and the single-tube reactor model is shown in Fig. 1(a).

Fig. 1(b) shows the arrangement of temperature sensors inside the reactor. To accurately monitor the temperature, eight sensors are placed in the reforming tube at a certain distance apart. Red points indicate the temperature sensor placed in the center of the core, and blue indicates the temperature sensor placed in the inner wall of the tube. At the same time, to make the methanol-water vapor entering the catalyst reach the set temperature, four FeCrAl wire clusters were placed at the entrance of the reaction tube to promote the further temperature rise of the methanol-water vapor.

Besides the single tube reformer, there are electronic scales, methanol storage tanks, peristaltic pumps, evaporator (EVA), condensers, soap film flowmeters, dryers, bubblers, gas chromatography (GC), etc. in the reforming system. The specific models of the relevant experimental instruments are shown in Table 1.

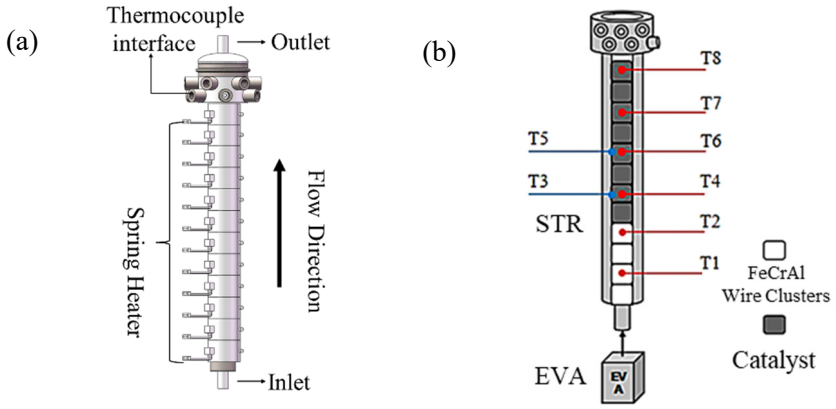

(a) Model of the single-tube reactor (b) The arrangement of temperature sensors

Fig. 1 The steam reformer

Table 1 The experimental instruments of the test system

	Equipment	Version	Manufacturers
1	Electronic Scales	JNS-6HWC	Hengzhifu Technology

2	Peristaltic Pump	BR100	Zibo Niukai
3	EVA & STR	/	Self-Innovate
5	Condenser	2000 mL	Lei Gu Technology
6	Soap Film Flowmeters	JCL-2010(S)-F	Qingdao Juchuang
7	GC	490 Micro GC	Agilent Technologies
8	Spring heater	30*50/K	OYG
9	Sheathed Thermocouple	KPS-IN600-ZG1/B	Kaipusen

The flow chart of the experiment is shown in Fig. 2. The experimental process is as follows: (1) heating the EVA and the STR, (2) pumping the methanol in the reactor with a peristaltic pump, (3) the methanol-water solution evaporates in the EVA and then reforming in STR, (4) condense the reforming gas in the condenser, (5) measure reformed gas flow rate with soap film flowmeters, (6) test the composition of reformed gas by GC, (7) test condensate composition by GC. The mass fraction of the methanol aqueous solution used in the experiment is 54.3%.

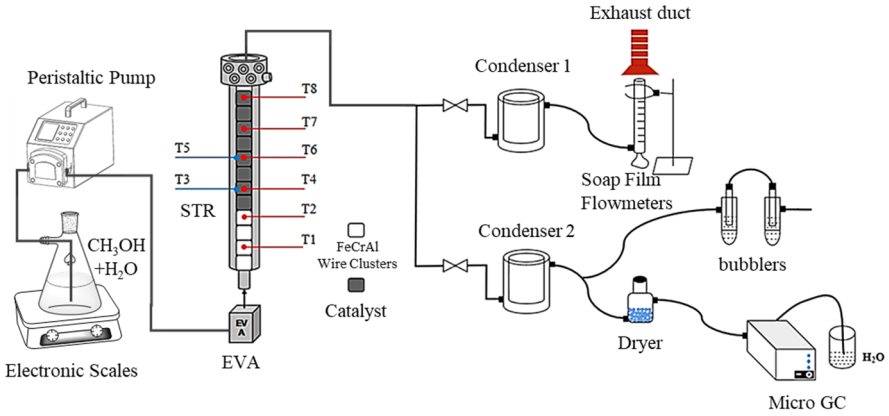

Fig. 2 The flow chart of the experiment

2.2 Catalyst and Principle

The main ingredient of the four different catalysts tested in this experiment is shown in Table 2. The WEF catalyst is a platinum-based catalyst that uses In_2O_3 as an auxiliary agent. The catalyzer is coated on the FeCrAl filament clusters. The BSF and CLN catalysts are graininess catalysts with CuO as the active constituent. Make ZnO the auxiliary agent and Al_2O_3 the support. Several materials are mixed and then pressed and sintered into catalyst particles. The active ingredient of the JSU catalyst is CuO, and the auxiliary agent is ZrO_2. The catalyst is attached to the Al_2O_3 ball by impregnation method inside the channel.

Table 2 Information on the catalysts

Catalyst	Active Ingredients	Accessory Ingredient	Carrier
WEF	Pt	In_2O_3	FeCrAl Wire
BSF	CuO	ZnO	Al_2O_3 Powder
CLN	CuO	ZnO	Al_2O_3 Powder
JSU	CuO	ZrO_2	Al_2O_3 Ball

All the catalysts for hydrogen generation of methanol-reforming studied in this paper are methanol steam reforming catalysts. Due to the intermediates in the methanol reaction process, the reaction is complicated. The study on the mechanism of methanol steam reforming has not reached a consensus. At present, the conclusion of the stream reaction mechanism is mainly five kinds. They are the methanol decomposition-water gas shift mechanism, methanol steam reforming-methanol decomposition mechanism, methanol steam reforming-water gas replacement inverse transformation mechanism, methanol steam reforming-decomposition-water gas shift mechanism, and reaction mechanism containing intermediate products. Taking the methanol steam reforming-decomposition-water gas shift mechanism as an example. The reaction mainly includes the following three processes:

Methanol Steam Reforming Reaction (MSR):

$$CH_3OH+H_2O \rightarrow CO_2+3H_2 \qquad \Delta^0_{298} = +49.4 \text{ kJ/mol} \qquad (1)$$

Methanol Decomposition Reaction (MD):

$$CH_3OH \rightarrow CO+2H_2 \qquad \Delta^0_{298} = +92.0 \text{ kJ/mol} \qquad (2)$$

Water Gas Shift Reaction (WGS):

$$CO+H_2O \rightarrow CO_2+H_2 \qquad \Delta^0_{298} = -41.4 \text{ kJ/mol} \qquad (3)$$

Equation (1) methanol steam reforming reaction and equation (2) methanol decomposition reaction is an endothermic reaction, and equation (3) water gas shift reaction is an exothermic reaction. When methanol is 100% converted into hydrogen, equation (1) can also be regarded as the total reaction formula of methanol steam

reforming reaction, and the whole reaction is endothermic [15-16].

2.3 Catalysts characterization

In this paper, the evaluation index of the performance of the catalysts is as follows: LHSV (h^{-1}) - the ratio of the volume of methanol-water injected per hour to the total volume of catalyst; methanol conversion rate (%) - the proportion of the amount of methanol consumed by the reaction to the total amount of methanol injected; hydrogen generation rate per unit volume Catalyst ($g/h \cdot cm^3_{cat}$) - the ratio of the mass of hydrogen generated per hour to the total catalyst volume; Catalyst hydrogen generation rate per unit mass ($g/h \cdot g_{cat}$) - the ratio of the mass of hydrogen generated per hour to the total catalyst mass; CO selectivity (%) - the molar amount of CO in dry gas versus the molar amount of $CO+CO_2$; bulk density of the catalysts (g/cm^3) - density obtained by dividing catalyst mass by the volume of the container occupied by the catalyst.

Many factors may affect the methanol-reforming reaction, including water-alcohol ratio, reaction temperature, LHSV, catalyst type, etc. So, we should confirm the parameters before the study. Firstly, the molar ratio of water to methanol is fixed as 1.5 (methanol aqueous solution with 54.3% mass concentration) based on previous experience. Then fix an appropriate LHSV, test the catalyst at different temperatures, and obtain the optimum reaction temperature. Finally, analyze the performance of each catalyst under the optimum reaction temperature and different LHSVs.

3. Test Results and Discussion

3.1. Bulk Density of the catalyst

Fig. 3 shows the bulk density of the four catalysts. CLN catalyst has the highest density, which is 1.601 g/cm^3. The bulk density of the WEF catalyst is 0.799 g/cm^3, which is the minimum. The bulk density of the catalyst can affect the volume and weight of the reformer. If the performance is consistent at the same LHSV, the catalyzer with a smaller bulk density is more dominant.

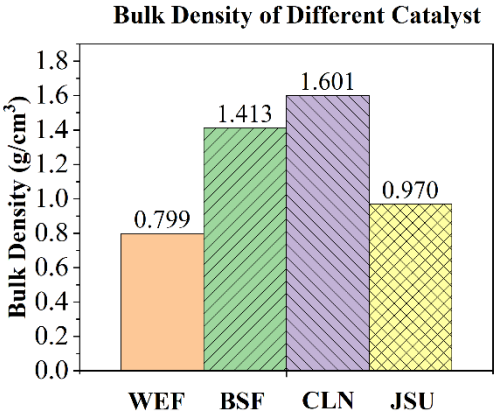

Fig. 3 Bulk densitiy of different catalyst

3.2. Methanol conversion rate

After a series of tests, the optimized reaction temperature of the catalysts was confirmed. The optimal reaction temperature range of the WEF catalyst was 325~375 ℃. The optimal reaction temperature range of the BSF, CLN, and JSU catalysts was 225~285 ℃. And the following study was tested under the same conditions. Fig. 4 shows the methanol conversion rate of four catalysts at different LHSVs. First, the methanol conversion rate decreases with the increase of LHSV. The main reason is that the increasing reactant increases the airspeed in the tube, and the average contact time between reactant and catalyst decreases, leading to a decrease in conversion rate. The catalyst with the highest methanol conversion rate was the BSF catalyst (95.38% in 8.6 h^{-1} LHSV, 97.90% in 7.55 h^{-1} LHSV), followed by the WEF, CLN, and JSU catalysts. The methanol conversion rate of the WEF catalyst in 9.23 h^{-1} LHSV is 91.83%, and 96.74% in 7.72 h^{-1} LHSV. CLN catalyst at an LHSV of 8.79 h^{-1} has a methanol conversion rate of 82.87%. The methanol conversion rate for the JSU catalyst at an LHSV of 6.21 h^{-1} is 59.64 %.

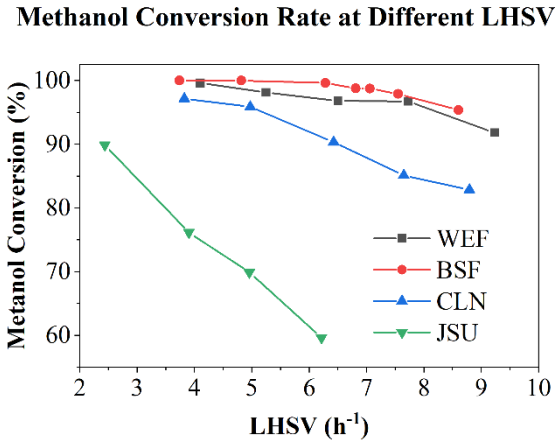

Fig.4 Methanol conversion rate at different LHSV

3.3. Hydrogen generation rate

Fig. 5(a) shows the hydrogen generation rates based on different LHSVs. Firstly, with the increase of LHSV, the hydrogen generation rate of the catalyst increases. The chemical reaction moves in forward because of the addition of reactants. Moreover, the LHSV in the test has not reached the maximum reactivity of the catalyst. As may be seen from the diagram, the BSF and WEF catalysts have the highest hydrogen generation capacity. At an LHSV of 4~7 h^{-1}, the capacity of hydrogen generation for the BSF catalyst is slightly higher than that of the WEF catalyst. At an LHSV within 7~9 h^{-1}, the hydrogen generation capacity of the BSF and WEF catalyst is almost the same. The hydrogen generation capacity of CLN and JSU catalysts ranked third and fourth. At an LHSV of 8.60 h^{-1}, the hydrogen generation rate of the BSF catalyst is 0.755 g/h·cm^3_{cat}. The hydrogen generation rate of the WEF catalyst at LHSV 9.23 h^{-1} is 0.779 g/h·cm^3_{cat}. CLN catalyst at LHSV 8.79 h^{-1} is 0.637 g/h·cm^3_{cat}. The JSU catalyst has the lowest catalytic performance. At LHSV of 6.21 h^{-1}, the hydrogen generation rate is 0.328 g/h·cm^3_{cat}.

The study aimed at studying the methanol-reforming catalysts applied onboard. So, the weight of the catalyst is also a consideration. The hydrogen generation capacity of the catalyst per unit mass under different LHSVs is shown in Fig. 5(b). As seen from the figure, the WEF catalyst has the highest hydrogen generation capacity per unit mass catalyst. The hydrogen generation rate of the catalyzers at 9.23 h^{-1} is 0.122 g/h·g_{cat}. The BSF, JSU, and CLN catalysts decreased. The changed phenomenon concerning the hydrogen generation per unit volume of catalysts, mainly because the density of catalysts was quite different. At LHSV of 8.60 h^{-1}, the hydrogen generation rate of the BSF catalyst per unit mass is 0.067 g/h·g_{cat}. At LHSV of 6.21 h^{-1}, JSU has a performance of 0.042 g/h·g_{cat}. The hydrogen generation rate of the CLN catalyst at LHSV 8.79 h^{-1} is 0.050 g/h·g_{cat}.

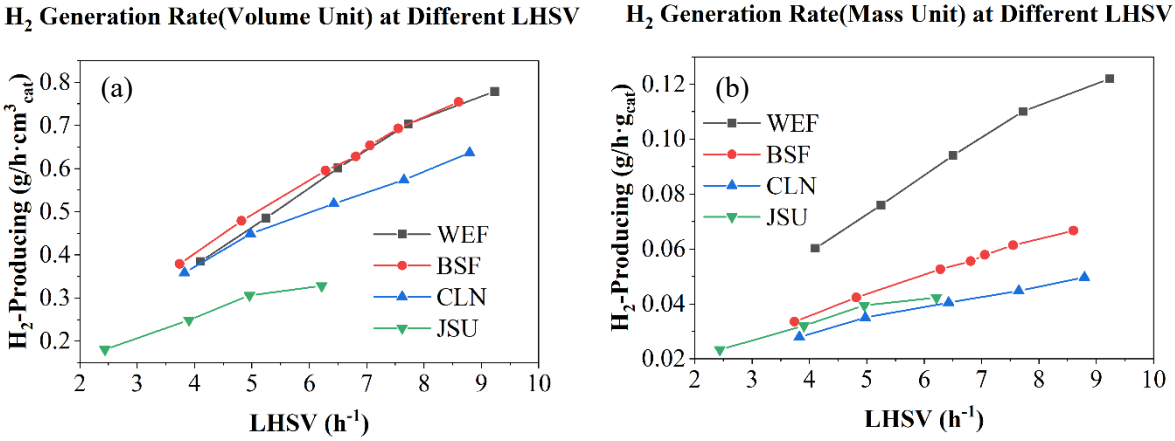

(a) Based on per unit volume of catalyst (b) Based on per unit mass of catalyst

Fig. 5 Hydrogen generation rate of four catalysts at different LHSVs

3.4. CO Selectivity

FIG. 8 shows the gas components of reformed gas generated by different catalysts at different LHSVs. Fig. 8(a) shows the CO content in reformed dry gas (excluding methanol and water), and Fig. 8(b) shows the CO selectivity. The reaction temperature has a significant effect on the content of CO in the reforming gas. The average temperature is taken and recorded in the data chart. The CO content in the dry gas of the WEF catalyst is the highest. Under the working temperature of 330 °C, the average CO content in the dry gas at different LHSVs is 4.61% and the average CO selectivity is 4.38%. The CO content of the BSF, CLN, and JSU catalysts decreased successively, and the CO selectivity has a similar pattern. The average working temperature with

CO content and CO selectivity of the BSF, CLN, and JSU catalysts were 255℃ - 2.28% - 4.18%, 285℃ - 1.64% - 3.54%, and 275℃ - 0.76% -2.67%, respectively. The main reason for the difference in CO content and CO selectivity in reforming gas is the temperature difference of the reforming reaction. Because there is a WSG process in the methanol steam reforming reaction, this reaction is exothermic. When the temperature rises, the chemical balance moves in the opposite direction, resulting in the rise of CO content.

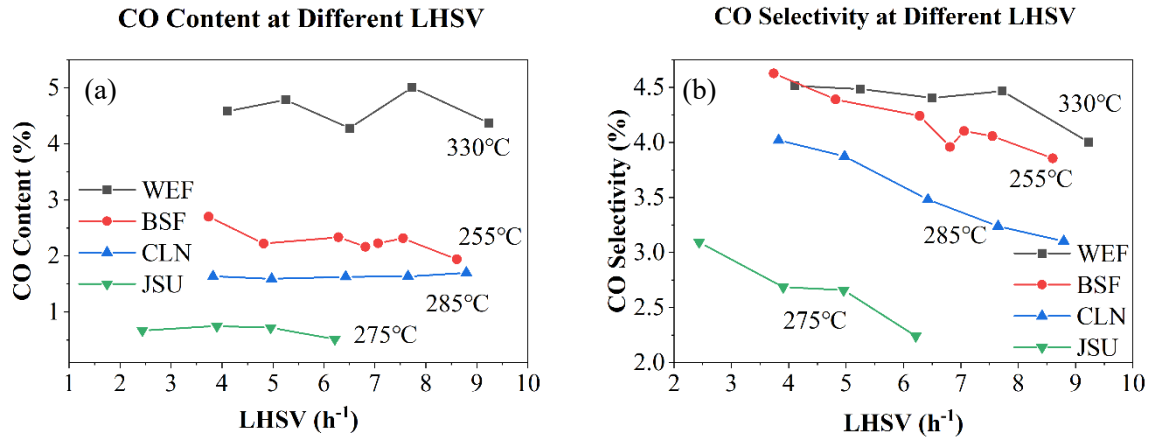

(a) CO content at a different LHSV (b) CO selectivity at a different LHSV

Fig. 6 Components of the dry reforming gas

4. Conclusion

This study compared the physicochemical properties and the catalytic performance of four catalysts. Based on the results and discussions presented above, the conclusions are obtained as below:

(1) The hydrogen generation rate per unit mass of the WEF catalyst is the highest. The hydrogen generation rate of the catalyzers in 9.23 h^{-1} is 0.122 g/h·g_{cat}, which can better meet the lightweight requirements of mobile devices. The methanol conversion rate is 91.83% in this condition. And the methanol conversion rate can reach 96.74% in 7.72 h^{-1} LHSV. At the same time, the WEF catalyst is coated on the FeCrAl filament clusters. So, its vibration resistance is excellent. Meanwhile, it has some disadvantages: the operating temperature is too high, and the CO content is almost twice as much as copper-based catalysts. The features make it more suitable for use in hydrogen combustion engines.

(2) The BSF catalyst with the highest methanol conversion rate (95.38% in 8.6 h^{-1} LHSV, 97.90% in 7.55 h^{-1} LHSV). However, because of the higher bulk density, the hydrogen generation rate per unit mass reached only 0.067 g/h·g_{cat} in 8.60 h^{-1}. The BSF catalyst is a copper-based granular catalyst and its disadvantage is easily sintering and powdering. It is more suitable for use in fixed equipment.

(3) CLN catalyst has no outstanding performance. The methanol conversion rate at an LHSV of 8.79 h^{-1} is 82.87%. Its formulation is similar to the BSF catalyst. It will also suffer sintered and pulverized.

(4) JSU catalyst adopts an alumina ball as support, so it has high hardness, which is very suitable for mobile equipment. But its catalytic performance needs to be improved. At an LHSV of 6.21h^{-1}, the methanol conversion rate is 59.64 %, and the hydrogen generation rate is 0.328 g/h·cm^3_{cat}.

Subsequent research should focus on the following two points: (1) optimize the reaction temperature of platinum-based catalysts and then develop low-temperature noble metal catalysts, thus reducing the difficulty of application in mobile devices. As well as reduce the concentration of CO in the reformed gas and expand their application; (2) improve the durability of copper-based catalysts and develop methanol reforming catalysts with high hardness, durability, and catalytic activity.

Acknowledgments

This work was financially supported by the Shanghai Science and Technology Commission's "Science and Technology Innovation Action Plan" high-tech field project (19511108200) and the 2021 Innovative and Entrepreneurial Talent Project of Jiangsu Province (JSSCRC2021330).

References

1. Dincer, I., & Zamfirescu, C. (2011). Sustainable energy systems and applications. Springer Science & Business Media.
2. Dutta, S. (2014). A review on production, storage of hydrogen and its utilization as an energy resource. Journal of Industrial and Engineering Chemistry, 20(4), 1148-1156.
3. Sá, S., Silva, H., Brandão, L., Sousa, J. M., & Mendes, A. (2010). Catalysts for methanol steam reforming—A review. Applied Catalysis B: Environmental, 99(1-2), 43-57.
4. Ayodele, B. V., Yassin, M. Y. B. M., Naim, R., & Abdullah, S. (2019). Hydrogen production by thermo-catalytic conversion of methane over lanthanum strontium cobalt ferrite (LSCF) and αAl2O3 supported Ni catalysts. Journal of the Energy Institute, 92(4), 892-903.
5. Luo, X., Hong, Y., Zhang, H., Shi, K., Yang, G., & Wu, T. (2019). Highly efficient steam reforming of

ethanol (SRE) over CeOx grown on the nano NixMgyO matrix: H2 production under a high GHSV condition. International Journal of Energy Research, 43(8), 3823-3836.

6. Garcia, G., Arriola, E., Chen, W. H., & De Luna, M. D. (2021). A comprehensive review of hydrogen production from methanol thermochemical conversion for sustainability. Energy, 217, 119384.
7. Ogden, J. M., Kreutz, T. G., & Steinbugler, M. M. (2000). Fuels for fuel cell vehicles. Fuel Cells Bulletin, 3(16), 5-13.
8. Li, H., Ma, C., Zou, X., Li, A., Huang, Z., & Zhu, L. (2021). On-board methanol catalytic reforming for hydrogen Production-A review. International Journal of Hydrogen Energy, 46(43), 22303-22327.
9. Chen, W. H., & Syu, Y. J. (2011). Thermal behavior and hydrogen production of methanol steam reforming and autothermal reforming with spiral preheating. International journal of hydrogen energy, 36(5), 3397-3408.
10. Fasanya, O. O., Al-Hajri, R., Ahmed, O. U., Myint, M. T., Atta, A. Y., Jibril, B. Y., & Dutta, J. (2019). Copper zinc oxide nanocatalysts grown on cordierite substrate for hydrogen production using methanol steam reforming. International Journal of Hydrogen Energy, 44(41), 22936-22946.
11. Zhao, J., Zhang, G., Liu, H., Shu, Q., & Zhang, Q. (2022). Improved charge transfer and morphology on Ti-modified Cu/γ-Al2O3/Al catalyst enhance the activity for methanol steam reforming. International Journal of Hydrogen Energy, 47(42), 18294-18304.
12. Chen, M., Sun, G., Wang, Y., Liang, D., Li, C., Wang, J., & Liu, Q. (2022). Steam reforming of methanol for hydrogen production over attapulgite-based zeolite-supported Cu-Zr catalyst. Fuel, 314, 122733.
13. Liu, L., Lin, Y., Hu, Y., Lin, Z., Lin, S., Du, M., ... & Wang, Y. (2022). ZnAl2O4 spinel-supported PdZnβ catalyst with parts per million Pd for methanol steam reforming. ACS Catalysis, 12(4), 2714-2721.
14. Kim, G. J., Kim, M. S., Byun, J. Y., & Hong, S. C. (2019). Effects of Ru addition to Pd/Al2O3 catalysts on methanol steam reforming reaction: A mechanistic study. Applied Catalysis A: General, 572, 115-123.
15. Kappis, K., Papavasiliou, J., & Avgouropoulos, G. (2021). Methanol reforming processes for fuel cell applications. Energies, 14(24), 8442.
16. Lytkina, A. A., Orekhova, N. V., & Yaroslavtsev, A. B. (2018). Catalysts for the steam reforming and electrochemical oxidation of methanol. Inorganic Materials, 54, 1315-1329.